Dynamic Eigenvector Centrality as a Biomarker for Motor Imagery Brain-Computer Interfaces

Paula G. Rodrigues
Engineering, Modeling and Applied Social Sciences Center
Federal University of ABC
São Bernardo do Campo, Brazil
ORCID: 0000-0002-5770-8558

Arnaldo Fim Neto
Engineering, Modeling and Applied Social Sciences Center
Federal University of ABC
São Bernardo do Campo, Brazil
ORCID: 0000-0002-4461-5416

André Kazuo Takahata
Engineering, Modeling and Applied Social Sciences Center
Federal University of ABC
Santo André, Brazil
ORCID: 0000-0002-7701-6452

Diogo C. Soriano
Engineering, Modeling and Applied Social Sciences Center
Federal University of ABC
São Bernardo do Campo, Brazil
ORCID: 0000-0002-9804-7477

Slawomir J. Nasuto
Biomedical Sciences and Biomedical Engineering Division
University of Reading
Reading, United Kingdom
ORCID: 0000-0001-9414-9049

Abstract— **Brain functional connectivity relies on the evaluation of instantaneous similarity between different brain regions. This strategy has been widely applied in neuroscience using fMRI data in order to understand brain connectivity organization implicated in some of the main brain pathologies, such as Parkinson and Alzheimer's disease. Recently, some studies have shown that the functional connectivity evaluation by means of graph metrics, more specifically eigenvector centrality, offers improved task discrimination in motor imagery EEG-based brain-computer interfaces. Nonetheless, these studies considered the connectivity as a static phenomenon and did not take into account the dynamic behaviour of the motor imagery process, which could add relevant information to task discrimination, by the inclusion of the preceding imagery (intention) and post-imagery phases. This work presents a classification performance comparison between dynamic eigenvalue centrality and dynamic power during the motor imagery experiment with a methodology based on a sliding window feature extraction with Pearson correlation as a measure of functional connectivity and a template matching classification approach, including preceding and post-motor imagery intervals. The results indicate that eigenvalue centrality can offer a promising complementary feature to classical bandpower for MI classification in BCI systems.**

Keywords—brain-computer interface; dynamic functional connectivity; motor imagery; graph; graph signal processing;

I. INTRODUCTION

Brain-computer interfaces (BCI) provide alternative communication systems that aim to directly map brain activity into commands for external assistive devices without the need for natural communication pathways [1]. Among the main BCIs paradigms, the motor imagery (MI) probably stands for as the main asynchronous framework for codifying the user's intention [1], although its performance is often beset with technical challenges, such as exhaustive training and higher inter-subject variability, in contrast to e.g. steady-state visually evoked potentials (SSVEPs) BCIs [2], [3]. Moreover, MI requires a better understanding of complex physiological mechanisms involving a cognitive engagement for intention, action planning and decision-making [4]. More recently, MI BCIs have been suggested as an important paradigm for rehabilitation purposes both after stroke [5] and spinal cord injury [6].

Advancing the design of motor imagery-based BCIs requires a better comprehension of the motor intention/imagery process, which includes identification of new biomarkers (or features) to classical event-related (de)synchronization (ERD/ERS) phenomena [7] for designing more robust classification schemes. Alternative methods for investigating brain activity have emerged in context of graph signal processing. This framework allows to evaluate the instantaneous similarity between different brain regions' activations under specific mental tasks – the brain functional connectivity (FC) - or even causal relations between such regions – the effective connectivity [8], [9]. FC evaluation has been successfully used in characterizing and diagnosing the main brain pathologies, including Parkinson's disease, Alzheimer's disease, Attention-Deficit/Hyperactivity Disorder (ADHD), or epilepsy [10]–[12]. Due to these achievements, FC graph analysis has also been applied for brain imaging modalities with better temporal resolution (e.g. EEG and MEG) for BCIs applications [13]–[15].

In particular, recent works dealing with FC analysis devoted to BCI systems [13], [14] have shown that graph eigenvector centrality (EC) defines an interesting and computationally efficient strategy for capturing MI networks. However, these studies have been performed under a single FC evaluation for the entire MI time interval and did not consider the possible role of preceding MI and post-MI processes, which may add relevant information to the discrimination process by taking into account motor intention and post-synchronization phenomena. Besides that, the dynamics underlying the FC along the MI process has not been considered, while it may play a key role for increasing the classification accuracy [16], [17].

This work presents a performance evaluation for binary classifications (MI right vs. left hand) using features based on dynamic eigenvalue centrality and dynamic power during the process of MI including the preceding and post-MI phases. The BCI competition IV dataset 2a was used given its widespread use in the literature, being just the C3 and C4 electrodes' connectivity considered for feature extraction due to their relation with the MI process. Classification performance was obtained based on a template matching approach taking into account the whole dynamics of the MI process.

II. MATERIAL AND METHODS

A. Database and EEG data processing

A benchmark online BCI-MI database (BCI Competition IV - dataset 2a) containing training and evaluation datasets for nine subjects was analyzed. Signals were recorded with 22 Ag/AgCl electrodes (Fz, FC3, FC1 ,FCz, FC2, FC4, C5, C3, C1, Cz, C2, C4, C6, CP3, CP1, CPZ, CP2, CP4, P1, PZ, P2, POz), sampled at 250 Hz and band-pass filtered between 0.5 and 100 Hz, being training and evaluation datasets (six sessions) acquired on different days. Training and evaluation sessions presented 12 trials for each MI task. We considered only right- and left-hand imagery tasks, resulting in 24 trials per session and 144 throughout the experiment. These trials lasted around 8 s, with 3 s being related to the MI preceded by a cue 1 s before. Details can be found in [18].

During offline processing, a Common Average Reference (CAR) spatial filter was applied to remove common electrodes' artifacts and the resulting signal was bandpass filtered between 8 and 30 Hz to enhance MI activity in mu and beta band due to frequency-dependent of ERD/ERS phenomenon [7]. All the processing routines were developed in Matlab 2015b.

B. Dynamic Functional Connectivity

The dynamic functional connectivity was computed by using a sliding window (SWD) of 0.5 s, for the entire trial duration (i.e. 8 s). Taking into account the 22 electrodes available, the pairwise connectivity was estimated by means of the Pearson correlation coefficient, traditionally applied in functional connectivity evaluation and used in [14] in the same dataset, and, afterwards, only the positive correlation values were considered in the weighted connectivity matrix.

Eigenvector centrality (EC) was chosen to characterize the relationship between electrodes due to its promising performance [14]. This graph metric considers not only the network structure around a node (electrode), but also considers the importance of its neighbours in the network [9]. Thus, each point of the time series was characterized by a graph EC value related to the electrodes' connectivity within the SWD. The definition of eigenvector centrality is presented in Eq. 1, in which λ is the largest eigenvalue of A and x_j are the respective eigenvectors [19].

$$EC_i = \frac{1}{\lambda} \sum_{j=1}^{n} A_{ij} x_j \qquad (1)$$

The quality of the between-class separation based on individual electrodes' eigenvector centralities was evaluated by the Fisher's discriminant ratio (FDR) for each sliding window. FDR is defined by the ratio of the distance between MI class centroids over their respective dispersions (standard-deviations) [14], [20] for training data. After certifying that the motor cortex electrodes provide the best class separability, only C3 and C4 electrodes' attributes were considered in the classification due to their close relation with the MI process.

For comparison, the bandpower evolution was computed using the same SWD. ERD/ERS was estimated for a better comparison with EC dynamics (Figure 4), but just instantaneous power was used as feature, since EC is not normalized by a baseline. For ERD/ERS evaluation, besides the previous band-pass filtering (8–30 Hz), the squaring of the amplitude samples was taken and the averaging of power

samples across all trials was evaluated. Finally, normalization by the power baseline was performed as presented in [7], [17].

C. Classification

For classifier training, right-hand and left-hand time-courses templates for electrodes C3 and C4 were obtained both for EC and bandpower features using exclusively the training dataset available for each volunteer. EC template for each electrode was obtained using the median of the EC computed for each SWD along the training trials. The EC median time course was then smoothed by a moving average of 10 points. The same procedure was performed for bandpower template evaluation, but considering the power for each SWD. Figure 1 illustrates a template for the electrode C3 for EC and bandpower approaches.
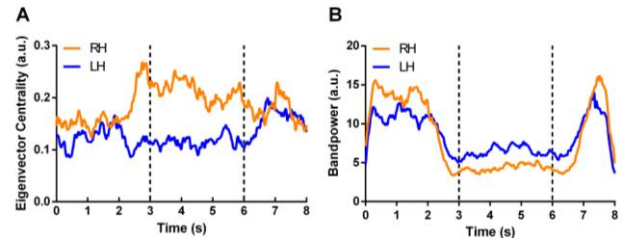

Fig. 1. Time course template of electrode C3 for eigenvector centrality (A) and bandpower (B). RH= right hand and LH = left hand task.

Classification was assessed on the evaluation dataset and was based on the minimum mean square error between a given trial time course of EC (or bandpower) and the respective (right- and left-hand) templates. This strategy considered the whole dynamics of the MI process by comparing the obtained feature for each SWD trial with a reference template for a given class and electrode [20]. The process is repeated for each volunteer and classification performance characterized by mean ± standard deviation.

III. RESULTS

Aiming to illustrate the role of motor cortex activity along the MI process, the FDR was computed for each volunteer using the training dataset to evaluate the time-course of the EC discrimination quality. It is noteworthy that the somatosensory area is essential to discriminate the mental tasks for one subject with a relatively-good MI performance (Fig. 2, left panel: period of 3 - 6 s). It can also be noted, that the increase of the discrimination quality occurs ~ 0.5 s after cue appearance, suggesting the role of motor intention as previously described [16].
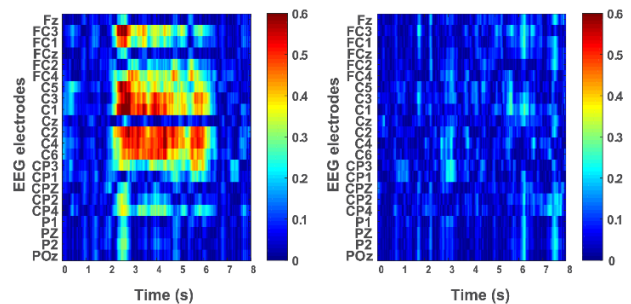

Fig. 2. Evolution of the time course of MI class separation based on electrodes' EC, measured by FDR, on training dataset. FDR time courses of 2 subjects before MI (0 - 2 s), during cue appearance (~2 - 3 s), during (3 - 6 s) and after MI (6 - 8 s). Notably, during MI (i.e. 3 - 6 s) good-performance volunteers (left panel – subject 3) exhibit higher FDR in the somatosensory cortex electrodes (e.g. C1, C3, C4, C6) then bad-performance volunteers (right panel – subject 2).

Visually, the left hemisphere electrodes C1, C3 and C5 were the best for discriminating the mental tasks, followed by the right hemisphere electrodes C2, C4 and C6. In contrast, for other subjects (Fig. 2, right panel), the FDR value remained practically unchanged during MI in comparison to baseline (i.e. 0 - 2 s before MI).

Analysis considering just C3 and C4 EEG electrodes were carried out to be in agreement with previous studies (e.g. [17]). The FDR time-course of EC and bandpower of a typical good-performance MI volunteer (subject 3) is shown in Fig. 3. It can be noticed that FDR monotonically increased during the cue appearance, highlighting the intention of MI task. Overall, during cue and MI the FDR values for EC were sustained higher than those obtained by bandpower feature.
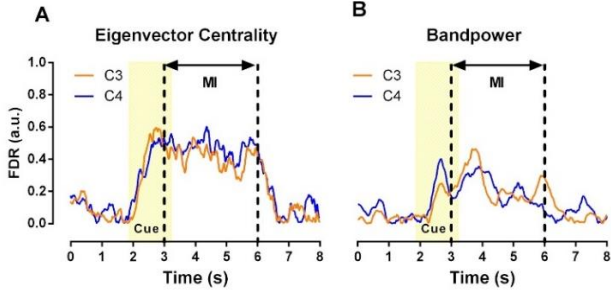

Fig. 3. Temporal evolution of FDR for Eigenvector centrality (A) and bandpower (B) before (0 - 2 s), during cue appearance (~2 - 3 s), MI (3 - 6 s) and after MI (6 - 8 s).

Figure 4 shows the subject' EC and ERD/ERS power time-course templates or C3 and C4 electrodes. EC enhancement occurs during cue appearance in contralateral electrodes (i.e. C3 for right hand MI and C4 for left hand MI) in contrast to ipsilateral electrodes (i.e. C4 for right hand MI and C3 for left hand MI), in which this graph metric decrease and kept sustained lower than the opposite electrodes during MI. After the mental tasks, no discrepancy between the temporal courses was observed. In addition, during MI, the ERD phenomenon was observed as previously shown in [17] followed by ERS occurrence.
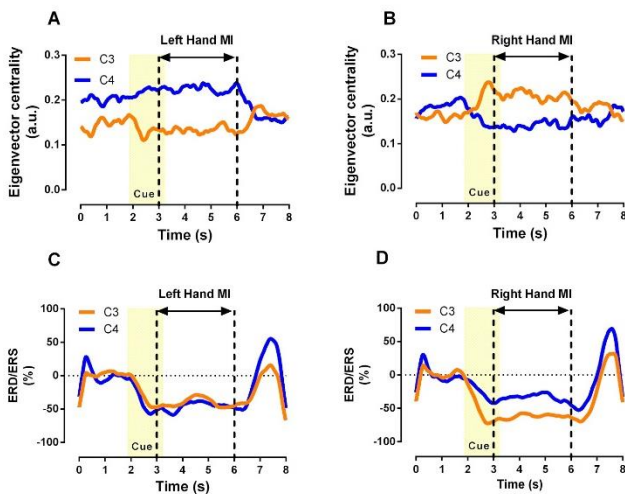

Fig. 4. Mean EC (A and B) and ERD/ERS (C and D) time-courses templates for C3 and C4 electrodes after smoothing (subject 3). For each painel, the cue interval (2 - 3 s) of the corresponding MI (3 - 6 s) is shown.

Table 1 shows the classification accuracy based on EC of C3, C4, their combination, and the bandpower. Considering C3 and C4 combination, the subjects with the best results - i.e.

accuracy higher than 0.7 - for EC were 1, 3 and 8. For bandpower, the best subjects were 7, 8 and 9. There were no statistically significant differences between the approaches when all subjects were considered (paired t-test).

TABLE I.   CLASSIFICATION ACCURACY FOR SUBJECTS CONSIDERING C3 AND C4 ELECTRODES AND THEIR COMBINATION REGARDING THE EIGENVECTOR CENTRALITY (EC) AND BANDPOWER (BP). MEAN ± STANDARD DEVIATION (SD).

Subj.	C3		C4		C3 plus C4	
	EC	BP	EC	BP	EC	BP
1	0.784	0.569	0.701	0.597	0.798	0.590
2	0.548	0.556	0.590	0.590	0.583	0.625
3	0.826	0.597	0.881	0.576	0.888	0.604
4	0.645	0.556	0.639	0.694	0.631	0.660
5	0.590	0.674	0.527	0.514	0.576	0.653
6	0.583	0.576	0.625	0.521	0.659	0.521
7	0.694	0.507	0.631	0.604	0.680	0.708
8	0.763	0.597	0.715	0.743	0.770	0.750
9	0.576	0.653	0.667	0.799	0.667	0.764
Mean ± SD	0.665 ± 0.100	0.587 ± 0.051	0.664 ± 0.099	0.626 ± 0.098	0.694 ± 0.104	0.653 ± 0.079

In addition, aiming to investigate whether both EC and bandpower may provide similar information, the Pearson correlation coefficient of their templates for either right or left hands MI was calculated for C3 and C4 electrodes. Typically, when the subject performed the MI task in the contralateral electrode, for instance, the C3 for right hand MI, the templates were anti-correlated, whereas in ipsilateral electrode (e.g. C4 for right hand MI) the correlation were mostly positives.

TABLE II.   CORRELATION OF THE EC AND BANDPOWER TEMPLATES. RH = RIGHT HAND AND LH = LEFT HAND.

Subj.	C3		C4	
	RH MI	LH MI	RH MI	LH MI
1	-0.645	-0.319	0.292	-0.374
2	-0.216	0.427	0.050	-0.029
3	-0.676	0.361	0.475	-0.694
4	0.076	0.421	-0.094	-0.225
5	-0.436	0.545	0.668	-0.301
6	-0.089	-0.008	0.338	-0.168
7	-0.782	-0.396	0.670	0.427
8	-0.496	0.078	-0.250	-0.600
9	-0.555	0.175	-0.304	-0.674

IV. DISCUSSION

In the present work, we aimed at extending the previous results reported in [14] on graph-based method EEG analysis by considering dynamic functional connectivity. Indeed, this approach as suggested in [15], [21] may provide a promising method of evaluation of the brain networks. Firstly, as expected, it was found that the electrodes over the somatosensory areas offer the best discrimination for the hand MI tasks. Using the C3 and C4 electrodes, the FDR increased within the time (~0.5 s) which may correspond to

movement intention as previously reported [4], and, then, kept higher during MI for both EC and bandpower in comparison to baseline period. Moreover, the temporal evolution of ERD/ERS was comparable to those reported to [17].

During classification process, in some subjects the accuracy exceeded 70% (e.g. subjects 1, 3 and 8) for EC and bandpower, but for others, the value was lower than 55%. It is possible that some subjects may not be able to perform the MI task as demonstrated in [22], which led previous investigators to consider only subjects with performance accuracy higher than 75% [17].

Moreover, although the accuracies found for EC and bandpower were not statistically different, it is reasonable to speculate that the information extracted by the both approaches are not exactly the same, since the Pearson correlations between the electrodes' templates were moderate in most cases for the good performance subjects, and the EC and bandpower accuracy levels were different for some subjects (e.g. 1, 3 and 8).

As a limitation of this study, we can mention the temporal dependency caused by the SWD and smoothing, that affects the accurate analysis of the transition between experimental phases. In addition, due to the characteristics of the MI experiment, it is difficult to ensure that the MI process is present only in the MI interval in the experimental protocol. Since the MI is an internal process, it is possible that some subjects have started the imagery soon after the cue appearance, which makes the analysis of the movement intention, or preceding MI engagement, a challenging task. Moreover, due to these transitions, the normality of the data cannot be assured. Despite that, Pearson correlation was able to estimate distinct functional connectivity patterns, as observed by the FDR and classification accuracy, justifying its use in this context.

V. CONCLUSION

This work presented an analysis of BCI-MI signals by means of the dynamic eigenvector centrality, which takes into consideration not only the information related to MI task – presented in the MI part of the experiment –, but also the dynamic related to the entire experiment, e.g. the dynamic transitions between the resting state and cue, etc. These results were compared to the dynamic power.

Regarding temporal analysis of the EC quality, we noticed that the most informative region relies on the MI interval (3 - 6 s), as expected. Moreover, we identified an increase in FDR related to the cue appearance, possibly related to the movement intention.

Finally, although not statistically significant, the classification results were promising, owing to the number of electrodes considered and the straightforward type of classification. The nature of the information extracted by the dynamic EC and power are likely not the same, what makes the combination of the approaches an interesting point for future investigation.

VI. ACKNOWLEDGEMENT

REFERENCES

[1]   J. R. Wolpaw, N. Birbaumer, D. J. McFarland, G. Pfurtscheller, and T. M. Vaughan, "Brain-computer interfaces for communication and control.," *Clin. Neurophysiol.*, vol. 113, no. 6, pp. 767–91, 2002.

[2]   M. Ahn and S. C. Jun, "Performance variation in motor imagery brain-computer interface: A brief review," *J. Neurosci. Methods*, 2015.

[3]   S. N. Carvalho *et al.*, "Comparative analysis of strategies for feature extraction and classification in SSVEP BCIs," *Biomed. Signal Process. Control*, vol. 21, no. AUGUST, pp. 34–42, Aug. 2015.

[4]   R. A. Andersen and H. Cui, "Intention, Action Planning, and Decision Making in Parietal-Frontal Circuits," *Neuron*, vol. 63, no. 5, pp. 568–583, Sep. 2009.

[5]   N. Sharma, V. M. Pomeroy, and J.-C. Baron, "Motor Imagery," *Stroke*, vol. 37, no. 7, pp. 1941–1952, Jul. 2006.

[6]   A. R. C. Donati *et al.*, "Long-Term Training with a Brain-Machine Interface-Based Gait Protocol Induces Partial Neurological Recovery in Paraplegic Patients," *Sci. Rep.*, vol. 6, no. 1, p. 30383, Sep. 2016.

[7]   G. Pfurtscheller and F. H. Lopes da Silva, "Event-related EEG/MEG synchronization and desynchronization: basic principles," *Clin. Neurophysiol.*, vol. 110, no. 11, pp. 1842–1857, Nov. 1999.

[8]   O. Sporns, *Networks of the Brain*. The MIT Press, 2011.

[9]   E. Bullmore and O. Sporns, "Complex brain networks: Graph theoretical analysis of structural and functional systems," *Nat. Rev. Neurosci.*, vol. 10, no. 3, pp. 186–198, 2009.

[10]   M. Díez-Cirarda *et al.*, "Dynamic functional connectivity in Parkinson's disease patients with mild cognitive impairment and normal cognition," *NeuroImage Clin.*, vol. 17, pp. 847–855, 2018.

[11]   C. Babiloni *et al.*, "Abnormalities of resting-state functional cortical connectivity in patients with dementia due to Alzheimer's and Lewy body diseases: an EEG study," *Neurobiol. Aging*, vol. 65, pp. 18–40, May 2018.

[12]   A. dos Santos Siqueira, C. E. Biazoli Junior, W. E. Comfort, L. A. Rohde, and J. R. Sato, "Abnormal Functional Resting-State Networks in ADHD: Graph Theory and Pattern Recognition Analysis of fMRI Data," *Biomed Res. Int.*, vol. 2014, pp. 1–10, 2014.

[13]   C. A. Stefano Filho, R. Attux, and G. Castellano, "Can graph metrics be used for EEG-BCIs based on hand motor imagery?," *Biomed. Signal Process. Control*, vol. 40, pp. 359–365, 2018.

[14]   P. G. Rodrigues, C. A. S. Filho, R. Attux, G. Castellano, and D. C. Soriano, "Space-time recurrences for functional connectivity evaluation and feature extraction in motor imagery brain-computer interfaces," *Med. Biol. Eng. Comput.*, May 2019.

[15]   I. Daly, S. J. Nasuto, and K. Warwick, "Brain computer interface control via functional connectivity dynamics," *Pattern Recognit.*, vol. 45, no. 6, pp. 2123–2136, Jun. 2012.

[16]   M. Wairagkar, Y. Hayashi, and S. J. Nasuto, "Exploration of neural correlates of movement intention based on characterisation of temporal dependencies in electroencephalography," *PLoS One*, vol. 13, no. 3, pp. 1–23, 2018.

[17]   F. Li *et al.*, "The Dynamic Brain Networks of Motor Imagery: Time-Varying Causality Analysis of Scalp EEG," *Int. J. Neural Syst.*, vol. 29, no. 01, p. 1850016, 2019.

[18]   M. Tangermann *et al.*, "Review of the BCI competition IV," *Front. Neurosci.*, vol. 6, no. JULY, pp. 1–31, 2012.

[19]   M. Newman, *Networks: An Introduction*. Oxford University Press, 2010.

[20]   S. Theodoridis and K. Koutroumbas, *Pattern Recognition*. Academic Press, 2009.

[21]   N. J. Williams, I. Daly, and S. J. Nasuto, "Markov Model-Based Method to Analyse Time-Varying Networks in EEG Task-Related Data," *Front. Comput. Neurosci.*, vol. 12, no. September, pp. 1–18, 2018.

[22]   M. H. Lee *et al.*, "EEG dataset and OpenBMI toolbox for three BCI paradigms: An investigation into BCI illiteracy," *Gigascience*, vol. 8, no. 5, pp. 1–16, 2019.